

MOVING LOADS - ANALYTICAL AND NUMERICAL APPROACHES¹

Bartłomiej DYNIEWICZ and Czesław BAJER

Institute of Fundamental Technological Research, Polish Academy of Sciences, Warsaw

1 Introduction

Nowadays problems with moving load are fundamental in transportation, since both loads and speed of travelling increase. Especially railway and bridge structures are affected by growing requirements. Dynamic effects in problems with moving load result in increased deformations. In the case of existing structures the load carrying capacity is a serious limit for real applications. There are two solutions: rebuild the structure or apply control system (with active, passive or semi-passive vibration damping). Such solutions have already been applied in experimental scale and in nature. However, the practical limit in the development of this technique is in the computational part of the project. Although limited complexity of the problem (usually reduced to constant travelling speed and simple set of massless or inertial loads) are intensively investigated, real problems with arbitrary loads and marching load function is still hardly treated.

Analytical solutions of beams and plates under travelling loads are widely presented in [1, 2, 3]. The reader can find there various problems treated analytically, with broad list of references. Numerical approach to the problem in the case of standing load can be found in numerous academic books. However, numerical treatment of the wave problem in the case of moving force and comparison to analytical solution is rarely published.

In the paper we intend to compare the accuracy and efficiency of two numerical approaches: discrete mesh method (for example the finite element method) and the meshless method (moving Galerkin least square method) [4]. Both approaches are related to the analytical solution. The basic set of problems to be investigated concerns moving massless and inertial force placed on the string and beam, without and with elastic foundation. In the present paper we limit our analysis to the string subjected to moving massless force and inertial force, without or with the Winkler foundation.

¹Supported by 4T12B 04829 grant

2 Constant moving force (analytical solution)

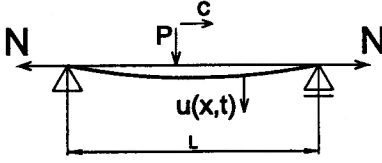


Figure 1: Constant moving force.

The point force moving with a constant speed c (Fig. 1) is introduced as the Dirac function $\delta(x)$. The motion equation then has the following form:

$$-N \frac{\partial^2 u(x,t)}{\partial x^2} + \rho A \frac{\partial^2 u(x,t)}{\partial t^2} = \delta(x-ct) P \quad (1)$$

N is the tensile force and ρA is the mass density per length. We impose boundary conditions

$$u(0,t) = 0 \quad u(l,t) = 0 \quad (2)$$

and initial conditions

$$u(x,0) = 0 \quad \left. \frac{\partial u(x,t)}{\partial t} \right|_{t=0} = 0. \quad (3)$$

Fourier transformation

The equation was solved with the use of operational calculus [5]. Antisymmetric part of the equation (1) was considered. It was written with sinus Fourier transform in the frequency domain. According to the sinus Fourier transform [6] we can get the transform of the equation (1):

$$\ddot{V}(j,t) + \omega_j^2 V(j,t) = \frac{P}{\rho A} \sin \omega t \quad (4)$$

where:

$$\omega = \frac{j\pi c}{l} \quad \omega_j^2 = \frac{j^2 \pi^2}{l^2} \frac{N}{\rho A}. \quad (5)$$

The Laplace-Carson transformation

In the equation (4) we go to the complex domain. In this case the solution is more simple. The L-C transformation [7] allows us to obtain

$$V^*(j,p) = \frac{P \omega}{\rho A} \frac{p}{p^2 + \omega^2} \frac{1}{p^2 + \omega_j^2}. \quad (6)$$

Inversion of Laplace-Carson transform

The inversion of L-C transform allows us to return to the real space (6):

$$V(j,t) = \frac{P}{\rho A} \frac{1}{\omega_j^2 - \omega^2} \left(\sin \omega t - \frac{\omega}{\omega_j} \sin \omega_j t \right). \quad (7)$$

The inversion of Fourier transform reduces the equation (7) to time domain:

$$u(x,t) = \sum_{j=1}^{\infty} \frac{2P}{\rho A l} \frac{1}{\omega_j^2 - \omega^2} \left(\sin \omega t - \frac{\omega}{\omega_j} \sin \omega_j t \right) \sin \frac{j\pi x}{l}. \quad (8)$$

We have the displacement $u(x,t)$ as the final solution of the equation.

3 Constant moving load with Winkler foundation (analytical solution)

The differential equation of the string with the Winkler foundation with constant stiffness k has a form:

$$-N \frac{\partial^2 u(x,t)}{\partial x^2} + \mu \frac{\partial^2 u(x,t)}{\partial t^2} + k u(x,t) = \delta(x-ct) P . \quad (9)$$

The solution of (9) is similar to the solution of the equation (1), with the following difference:

$$\omega_j^2 = \frac{j^2 \pi^2}{l^2} \frac{N}{\mu} + \frac{k}{\mu} . \quad (10)$$

4 Moving inertial load (analytical approach)

Displacement of the string under the moving inertial load (Fig. 2) can be written in the form:

$$u(x,t) = \int_0^l G(x,s) p(s,t) ds , \quad (11)$$

where $G(x,s)$ is the Green function. Inertial load $p(s,t)$ applied to the string is given by the function (12):

$$p(s,t) = \delta(x-ct) \left(P - m \frac{\partial^2 u(ct,t)}{\partial t^2} \right) \quad (12)$$

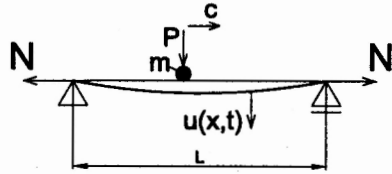


Figure 2: Moving inertial load.

4.1 Massless string

Assuming $\rho = 0$, $P = 1$ and $x = s$, the equation (1) after integration has a form:

$$u(x) = \frac{-1}{N} (H(x-s)x - H(x-s)s) + C_1 x + C_2 , \quad (13)$$

where $H(x-s)$ is the Heaviside function. Taking into account boundary conditions (2) we can solve for constants C_1 and C_2 .

We substitute:

$$x = ct \quad u_1(t) = u(ct,t) \quad (14)$$

Taking (11) and (12) with the constant force $P - m \frac{\partial^2 u(ct,t)}{\partial t^2}$, the problem is reduced to the computation of the integral Γ :

$$\Gamma = \int_0^l G(x,s) \delta(s-ct) ds . \quad (15)$$

Taking into account (14) we have:

$$\Gamma_1 = \Gamma_2 = \frac{1}{N} \left(1 - \frac{ct}{l} \right) ct = G(ct, ct) \quad (16)$$

and with (11), (12), (14) and (16) we have:

$$u_1(t) = \left(P - m \frac{\partial^2 u_1(t)}{\partial t^2} \right) \left[\frac{1}{N} \left(1 - \frac{ct}{l} \right) ct \right]. \quad (17)$$

Static displacement in the middle of the string length:

$$u_0 = \frac{Pl}{4N}. \quad (18)$$

By introducing (17) and (18) we have dimensionless displacements $y(\tau)$, and dimensionless time τ :

$$y(\tau) = \frac{u_1(t)}{u_0} \quad \tau = \frac{ct}{l}. \quad (19)$$

Substitution of (19) into (17) results in:

$$\tau(1-\tau)\ddot{y}(\tau) + 2\alpha y(\tau) = 8\alpha\tau(1-\tau), \quad (20)$$

where:

$$\alpha = \frac{Nl}{2mc^2}. \quad (21)$$

4.1.1 The case of $\alpha \neq 1$

We assume the equation

$$y(\tau) = \tau(1-\tau)\nu(\tau) \quad (22)$$

to be the solution of (20). Substitution of the function (22) and its second derivative into (20) we have:

$$\tau(1-\tau)\ddot{\nu}(\tau) + (2-4\tau)\dot{\nu}(\tau) - 2(1-\alpha)\nu(\tau) = 8\alpha. \quad (23)$$

The Eqn. (23) is the hypergeometric non-homogeneous one [8]. Its general form is given by the formula:

$$\tau(1-\tau)\ddot{\nu}(\tau) + [c - (a+b+1)\tau]\dot{\nu}(\tau) - ab\nu(\tau) = 0. \quad (24)$$

In the first stage we solve a homogeneous equation of the Eqn. (23). With the use of (24) we obtain the system of equations, which has the following solution:

$$a_{1,2} = \frac{3 \pm \sqrt{1+8\alpha}}{2} \quad b_{1,2} = \frac{3 \mp \sqrt{1+8\alpha}}{2} \quad c = 2. \quad (25)$$

The solution of the hypergeometric equation with c be a natural number $c = 1 + m$ and $a \neq m, b \neq m$:

$$\nu_1(\tau) = F(a, b, c, \tau)$$

$$\begin{aligned} \nu_2(\tau) = & F(a, b, c, \tau) \ln \tau + \sum_{k=1}^{\infty} \left\{ \frac{(a_k)(b_k)}{(c_k)} [h(k) - h(0)] \frac{\tau^k}{k!} + \right. \\ & \left. + \frac{1}{(1-a)(1-b)\tau} \right\}, \quad (26) \end{aligned}$$

where $F(a, b, c, \tau)$ is the hypergeometric series determined as:

$$F(a, b, c, \tau) = 1 + \sum_{k=1}^{\infty} \frac{(a_k)(b_k)}{(c_k)} \frac{\tau^k}{k!} \quad (27)$$

$$\begin{aligned} (a_k) &= a(a+1)\dots(a+k-1) \\ (b_k) &= b(b+1)\dots(b+k-1) \end{aligned} \quad (28)$$

$$h(k) = \psi(a+k) + \psi(b+k) - \psi(2+k) - \psi(1+k) \quad (29)$$

$$\psi(x) = -C - \frac{1}{x} + x \sum_{n=1}^{\infty} \frac{1}{n(x+n)} . \quad (30)$$

It means that α exists for which the solution (26) is not fulfilled. Particular solution of (23) is as follows:

$$\nu_s(\tau) = \frac{4\alpha}{\alpha-1} . \quad (31)$$

The complete solution of the equation (20) with the use of (22) is the equation:

$$y(\tau) = [A_1 \nu_1(\tau) + A_2 \nu_2(\tau) + \nu_s(\tau)] \tau(1-\tau) . \quad (32)$$

For the initial condition we can compute constants A_1 and A_2

$$A_1 = \frac{-4\alpha}{\alpha-1} \quad A_2 = 0 . \quad (33)$$

The constant $A_2 = 0$ results in the simplification of the formula (32). Finally the displacement of the string with $\alpha \neq 1$ is described by the relation

$$\begin{aligned} y(\tau) &= \frac{4\alpha}{\alpha-1} \tau(1-\tau) [1 - \nu_1(\tau)] \\ &= \frac{4\alpha}{\alpha-1} \tau(1-\tau) [1 - F(a, b, c, \tau)] , \end{aligned} \quad (34)$$

where $F(a, b, c, \tau)$ is given by (27).

4.1.2 The case of $\alpha = 1$

In the case of $\alpha = 1$ the equation (20) has a form:

$$\tau(1-\tau)\ddot{y}(\tau) + 2y(\tau) = 8\tau(1-\tau) \quad (35)$$

The first order equation below is one of two solutions of the Eqn. (35)

$$\tau(1-\tau)\dot{y}_1(\tau) - (1-2\tau)y_1(\tau) = 0 . \quad (36)$$

After integration

$$y_1(\tau) = \tau(1-\tau) \quad (37)$$

The second solution of (35):

$$y_2(\tau) = y_1(\tau)u(\tau) = \tau(1-\tau)u(\tau) \quad (38)$$

After differentiation and substitution of (38) into (35) we have:

$$\tau(1 - \tau)\ddot{u}(\tau) + 2(1 - 2\tau)\dot{u}(\tau) = 8 \quad (39)$$

We solve the homogeneous equation (39) substituting $u_1(\tau) = \dot{u}(\tau)$:

$$\tau(1 - \tau)\dot{u}_1(\tau) + 2(1 - 2\tau)u_1(\tau) = 0 \quad (40)$$

$$u_1(\tau) = [\tau(1 - \tau)]^{-2} \quad (41)$$

Finally the solution of (39) has a form:

$$u(\tau) = \frac{1}{1 - \tau} - \frac{1}{\tau} - 2 \ln \frac{1 - \tau}{\tau} \quad (42)$$

Then

$$y_2(\tau) = 2\tau - 1 - 2\tau(1 - \tau) \ln \frac{1 - \tau}{\tau} \quad (43)$$

Since the Wronski determinant $W \neq 0$, the equations $y_1(\tau)$ and $y_2(\tau)$, which are the integrals of the homogeneous equation are linearly dependent, the general solution of the equation (35) has a form

$$y(\tau) = A_1(\tau)y_1(\tau) + A_2(\tau)y_2(\tau) \quad (44)$$

Full solution of Eqn. (35) can be obtained with the use of variation of constant method, where

$$A_1 = \int \frac{-8y_2(\tau)}{W} d\tau \quad A_2 = \int \frac{8y_1(\tau)}{W} d\tau \quad (45)$$

With (37) and (43) we get:

$$\begin{aligned} A_1(\tau) &= -8 \left\{ \tau^2 - \tau^2 \ln \frac{1 - \tau}{\tau} + \ln(1 - \tau) + \right. \\ &+ \left. \frac{2}{3} \left[\tau^3 \ln \frac{1 - \tau}{\tau} - \frac{1}{2} (\tau + 2)\tau - \ln(1 - \tau) \right] \right\} + D_1 \\ A_2 &= \frac{4}{3} \tau^2 (3 - 2\tau) + D_2 \end{aligned} \quad (46)$$

Integration constants D_1 and D_2 can be computed from initial conditions (3) :

$$D_1 = 0 \quad D_2 = 0 \quad (47)$$

The final relation for displacement, which is the solution of Eqn. (35) has a form:

$$\begin{aligned} y(\tau) &= \frac{4}{3} \tau^2 (3 - 2\tau) \left[2\tau - 1 - 2\tau(1 - \tau) \ln \frac{1 - \tau}{\tau} \right] - \\ &- 8\tau(1 - \tau) \left\{ \tau^2 - \tau^2 \ln \frac{1 - \tau}{\tau} + \ln(1 - \tau) + \right. \\ &+ \left. \frac{2}{3} \left[\tau^3 \ln \frac{1 - \tau}{\tau} - \frac{1}{2} (\tau + 2)\tau - \ln(1 - \tau) \right] \right\} \end{aligned} \quad (48)$$

5 Meshless methods (Element Free Galerkin Method)

The idea of meshless methods is to eliminate the mesh generation stage, which is the main disadvantage of the finite element method (or other classical discrete methods). In the meshless method the set of separated points is placed in the domain of the structure. Interpolation functions (shape functions) are then generated not in element subdomains, but in arbitrary placed nodal points.

Below we consider a particular method of shape function generation, called Moving Least Square (MLS) method [4]. Shape functions are stretched on points being in the neighbourhood of the given point, in the stepping subdomain Ω . The interpolation error

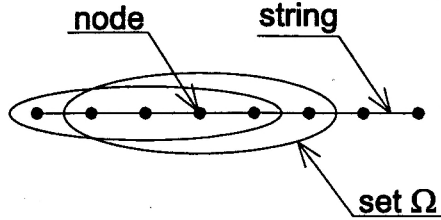


Figure 3: The set Ω moving along a string.

in MLS method is given by

$$J = \sum_{i=1}^n W(x - x_i) [u^h(x, x_i) - u_i]^2, \quad (49)$$

where $W(x - x_i)$ is the weight function, $u^h(x, x_i)$ is the polynomial of approximation, and u_i are nodal values. We assume exponential shape functions:

$$W(x - x_i) = \begin{cases} e^{-\left(\frac{x-x_i}{\alpha}\right)^2} & \text{if } (x - x_i) \leq 1 \\ 0 & \text{if } (x - x_i) > 1 \end{cases}. \quad (50)$$

The coefficient α depends on the size of the domain Ω and the number of points in the domain. In the uni-dimensional case

$$u^h(x, x_i) = \mathbf{p}^T(x_i)\mathbf{a}(x), \quad (51)$$

where monomials in the interpolation polynomial is

$$\mathbf{p}^T = (1, x, x^2, \dots), \quad (52)$$

with approximation coefficients

$$\mathbf{a}^T(x) = (a_0(x), a_1(x), a_2(x), \dots). \quad (53)$$

We minimize the interpolation error. J is minimized according to coefficients \mathbf{a} :

$$\frac{\partial J}{\partial \mathbf{a}} = \mathbf{0}. \quad (54)$$

Differentiation of (49) yields:

$$a(x) = A_1^{-1}(x) A_2(x) u_i \quad (55)$$

where:

$$A_1 = P^T W(x - x_i) P \quad A_2 = P^T W(x - x_i) \quad (56)$$

$$P = \begin{pmatrix} p_1(x_1) & p_2(x_2) & \cdots & p_m(x_n) \\ p_1(x_1) & p_2(x_2) & \cdots & p_m(x_n) \\ \vdots & \vdots & \ddots & \vdots \\ p_1(x_n) & p_2(x_n) & \cdots & p_m(x_n) \end{pmatrix} \quad (57)$$

Equations (51) and (55) lead to:

$$u^h(x, x_i) = \mathbf{p}^T(x_i) A_1^{-1}(x) A_2(x) u_i = \sum_{i=1}^n \phi_i^k(x) u_i \quad (58)$$

where $\phi_i^k(x)$ is the shape function and k is the degree of the approximation polynomial.

$$\phi_i^k = \mathbf{p}^T(x_i) A_1^{-1}(x) A_2(x) = [\phi_1^k(x), \phi_2^k(x), \dots, \phi_n^k(x)] \quad (59)$$

Since the inversion of the matrix \mathbf{A} in a general form can not be simply computed, the approximation of the zero degree of $\mathbf{p}^T = 1$ is applied in practice. Thus we obtain the so-called Shepard function:

$$\phi_i^0 = \frac{W(x - x_i)}{\sum_{i=1}^n W(x - x_i)} \quad (60)$$

Eqn. (60) and the differential equation of motion

$$\sigma_{ij,j} + b_i = \rho \ddot{u}_i \quad (61)$$

we can obtain the stiffness and inertia matrix:

$$k_{ij} = \int_{\Omega} B_i^T N B_j d\Omega$$

$$m_{ij} = \int_{\Omega} \phi_i^T \rho A \phi_j d\Omega, \quad (62)$$

where $B = \frac{\partial \phi}{\partial x}$, N - tensile force and ρ - mass density. Nodal matrices \mathbf{k} and \mathbf{m} computed for domains Ω are assembled in global matrices \mathbf{K} and \mathbf{M} . The proper choice of a parameter is still the fundamental problem (Eqn. 50).

6 Results

Numerical results are compared with analytical results. In the Fig. 4 we have plots of displacements under moving force and in the middle of the string length. The analytical solution well coincides with the one obtained with the finite element method or central difference method. The meshless method results in good approach of the accurate solution. In this method we can notice the phase error, visible especially in the second half of the observation period. It means that the rigidity is higher than required. However, smoothing effect is the main reason of differences of results. Significantly lower number of points in

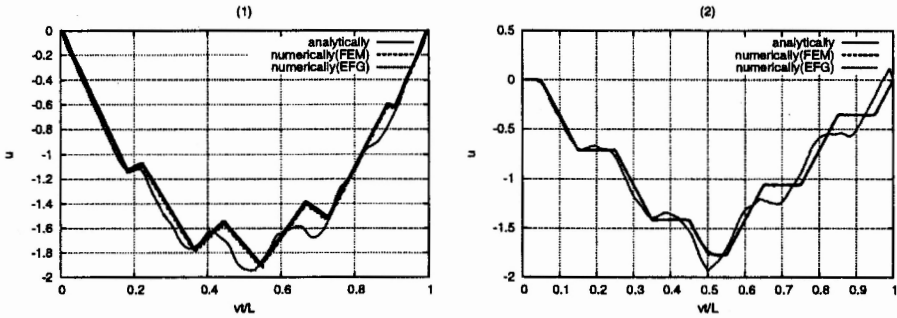


Figure 4: Displacements under constant moving force: (1) under moving force, (2) in the middle of the string length (number of points in Ω equal to 10).

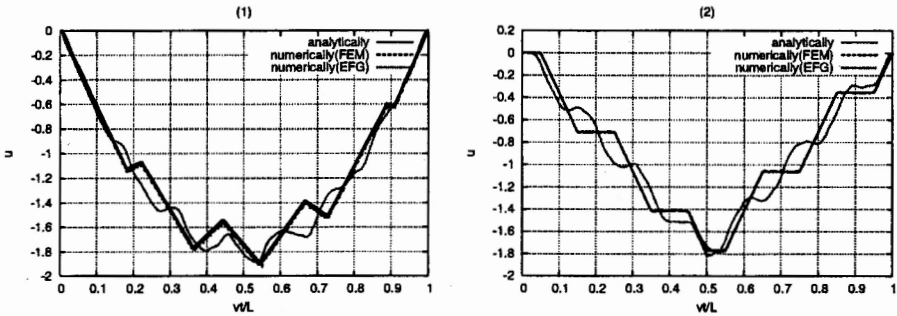


Figure 5: Displacements under constant moving force: (1) under moving force, (2) in the middle of the string length (number of points in Ω equal to 2).

the moving domain (2 instead of 10 as in the previous case) (Fig. 5) results in quite similar plots. Both the amplitude and the period of vibrations are acceptable.

The numerical approach in the case of Winkler foundation does not differ from the analytical solution. We must emphasize here, that continuously moving force in the numerical application is replaced with the sequence of marching pair of forces, applied to nodal points. In such a case we neglect mixed derivatives of the formulation. We can notice that such an analysis does not introduce significant error (Fig. 6).

Plots for the inertial load in the case of moving high mass (Fig. 7) differ with analytical ones. In the case of lower moving mass both lines coincide (Fig. 8). Higher speed does not allow to compare both analytical and numerical plots successfully (Fig. 8).

7 Conclusions

Analytical solutions fail in cases of high speed or high inertia of the moving force. Meshless methods are fast and can be successfully applied to the group of problems discussed in the paper.

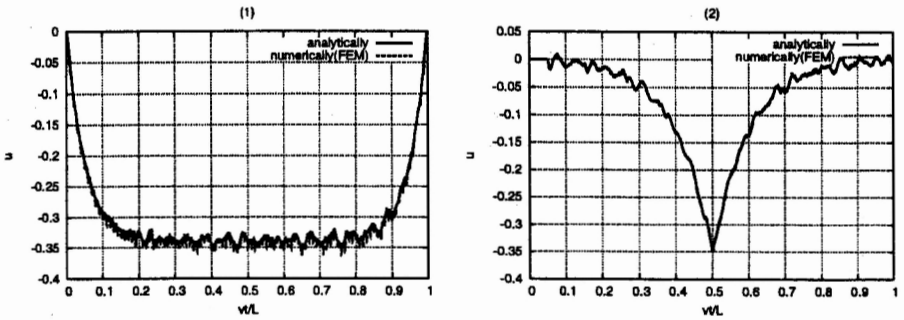


Figure 6: Displacements under constant moving force - string based on the Winkler foundation: (1) under moving force, (2) in the middle of the string length.

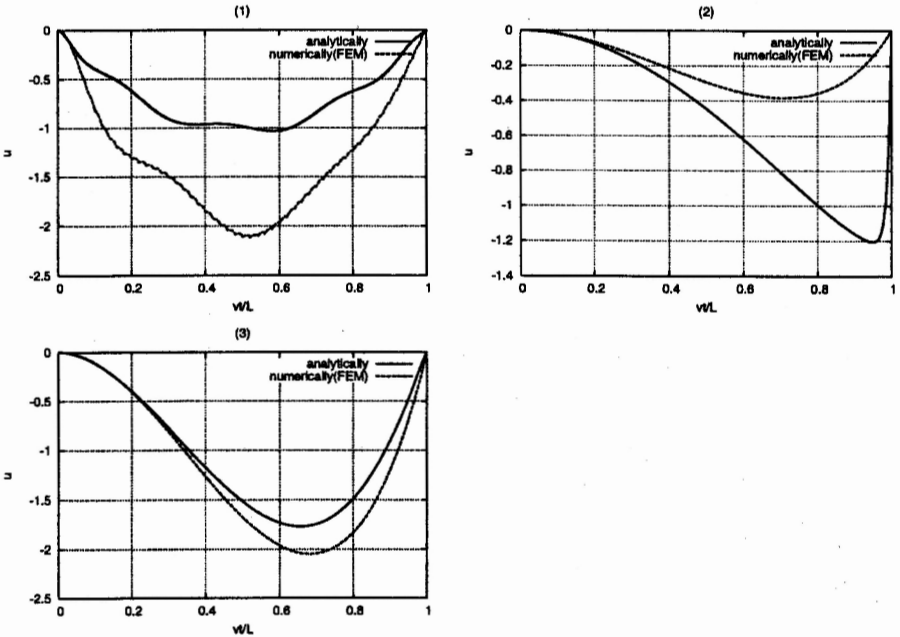


Figure 7: Inertial force (string mass/moving mass=1/1000), $\alpha \neq 1$; the speed: 1) $c = 0.01$; 2) $c = 0.1$; 3) $c = 0.04$.

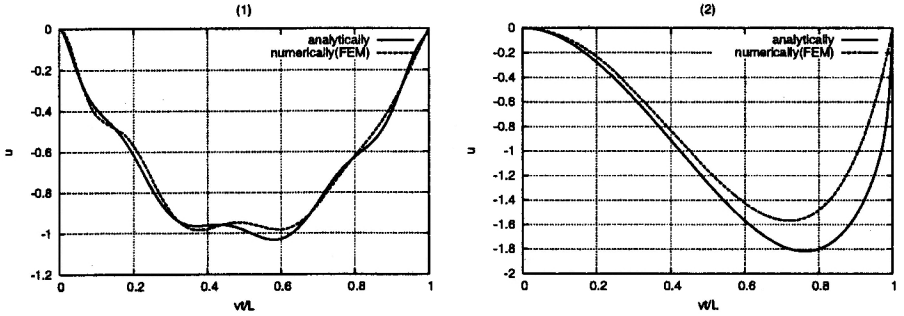


Figure 8: Inertial load with string mass/moving mass=1/10 ($\alpha \neq 1$) for different speed of the force. Left diagram: $v = 0.1$, right diagram: $v = 0.5$.

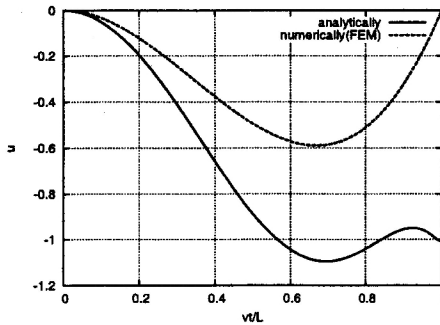


Figure 9: Inertial load, high moving speed ($\alpha = 1$)

References

- [1] L. Fryba. *Vibrations of solids and structures under moving loads*. Academia, Prague, 1972.
- [2] W. Szcześniak. Inercyjne obciążenia ruchome na belkach. *Prace Naukowe, Politechnika Warszawska, budownictwo* 112, 1990.
- [3] W. Szcześniak. Wybrane zagadnienia dynamiki płyt poddanych inercyjnym obciążeniom ruchomym. *Prace Naukowe, Politechnika Warszawska, budownictwo* 119, 1992.
- [4] T. Belytschko, Y. Krongauz, D. Organ, M. Fleming, and P. Krysl. Meshless methods: An overview and recent developments. *Comput. Methods Appl. Mech. Engrg*, 139(1-4):3-47, July 1996.
- [5] K. W. Wagner. *Rachunek operatorowy i przekształcenie Laplace'a*. PWN, Warszawa, 1960.
- [6] R. Bracewell. *Przekształcenie Fouriera i jego zastosowania*. WNT, Warszawa, 1965.
- [7] G. Doetsch. *Praktyka przekształcenia Laplace'a*. PWN, Warszawa, 1964.
- [8] J.B. Seaborn. *Hypergeometric functions and their applications*. Springer, New York, 1991.

RUCHOME OBCIĄŻENIA - ROZWINIĘCIA ANALITYCZNE I NUMERYCZNE

W pracy przedstawiono ocenę dokładności i skuteczności zastosowania metod numerycznych w zadaniach falowych. Metody analityczne są skuteczne w ograniczonym zakresie parametrów. Klasyczne metody numeryczne pozwalają uzyskać wysoką dokładność, choć wymagają znacznie większego wysiłku obliczeniowego niż metody bezsiatkowe. Te ostatnie pozwalają na obliczenia z zadawalającą dokładnością. Wyniki obarczone są nieznacznym błędem fazowym oraz charakteryzują się rozmyciem czoła fali.